Journal of the European Optical Society - Rapid Publications 6, 11004 (2011) www.jeos.org

Spectral properties for 1D multilayer systems and application to super resolution

A. Mandatori INFM at Dipartimento di Energetica Università La Sapienza di Roma Via Scarpa 16, 00161, Roma, Italy

M. Bertolotti INFM at Dipartimento di Energetica Università La Sapienza di Roma Via Scarpa 16, 00161, Roma, Italy
mario.bertolotti@uniroma1.it

The spectral properties of one-dimensional multilayer structures for the two polarizations TE and TM are investigated and a physical explanation for the large spatial transmission band that can be obtained with this kind of system is given together with a discussion of the correlated super resolution effect. A designing approach to build 1D metal-dielectric multilayer structures that have super resolution is also suggested. [DOI: 10.2971/jeos.2011.11004]

Keywords: super resolution, waveguide, metamaterials

1 INTRODUCTION

As first noted by Pendry [1], the evanescent waves restoring by an ideal negative index material (NIM) layer can lead to subwavelength resolution below the Rayleigh limit. This theoretical prediction was later confirmed by experiments carried out using a flat lens composed of a single silver layer 40-50 nm thick [2], [3]. This theory generally requires that the thickness of the metal film (about 5 nm) should be very small compared to the wavelength of the input signal. In fact, unlike an ideal, lossless NIM, which can amplify evanescent waves, silver can only slow down the rate of decay of the evanescent components: in terms of energy flow, the propagation is always characterized by losses. The source is thus generally placed very near to the flat metal lens, typically within $\lambda_0/5$-$\lambda_0/10$, where λ_0 is the incident wavelength. At such small distances, sub-wavelength resolution can also be obtained with near-field scanning optical microscopy [4], [5]. More recently, a new scheme was proposed to increase the distance where super resolution can still be observed [6]. Pendry et al. [7]–[9] have considered a multilayer structure that improves super-resolution in the near-field zone relative to the single metal layer. The structure consisted of eight periods of alternating metal and air layers that were assumed to have equal thickness (5 nm each). The incident wavelength was chosen in a way that the real parts of the permittivity would nearly balance each other, namely $\epsilon = 1$ for air, and $\epsilon \sim -1$ for silver. Excluding losses, these conditions are approximately satisfied for ultraviolet light in the range between 345 and 360 nm, slightly below the plasma frequency of silver ($\lambda_p \sim$ 320 nm). Although the layered structure displayed improved resolving capabilities, the overall transmittance of propagating modes was nearly identical to the transmittance from a single metal layer 40 nm thick, as originally proposed in [1]. One obvious drawback in the new system was the much reduced metal layer thickness, down to about 5 nm or so, which from a technological point of view is still quite a challenge to achieve. Another scheme that achieves super-resolution in metal-dielectric structures was recently proposed [10], [11] based on thick alternating layers arranged to produce a resonant structure, in a regime where effective medium theory is not applicable (in this scheme the thickness of the layers, about 40 nm, are not thin enough compared to the wavelength to allow the use of the effective medium approximation, as was done by Pendry for his thin structures). The structure in this case may not transmit evanescent waves and the main underlying physical mechanisms for sub-wavelength focusing are resonance tunnelling, field localization and propagation effects [11]. One important property is its spatial transmission spectrum. In the present paper we perform a study of multilayered structures that are able to exhibit super resolution: we demonstrate that this property is well related to the cavity properties of the structure and that it can involve every kind of 1D multilayer for every input field polarization. By properly choosing the geometry and the refractive index of the layers super resolution can be achieved. In the next Section we present a general discussion of the spatial transmission of unidimensional multilayers and its connection to super-resolution. Section 3 considers the possibility to improve resolution, and the final Section 4 presents some design criteria to optimize the structure for super-resolution. Conclusions close the paper.

2 SPECTRAL PROPERTIES

Before starting to investigate super resolution in a 1D multilayer structures and the physical explanation of this phenomenon, we want to discuss about some properties of the Fourier transform and of the transfer function of a linear system made by a one-dimensional photonic band gap (PBG) sample. Between the input $V_i(k_x)$ and the output field $V_o(k_x)$ in the transformation domain where k_x is the wavevector component in the x direction which is normal to structure axis

Received March 22, 2010; published February 22, 2011 ISSN 1990-2573

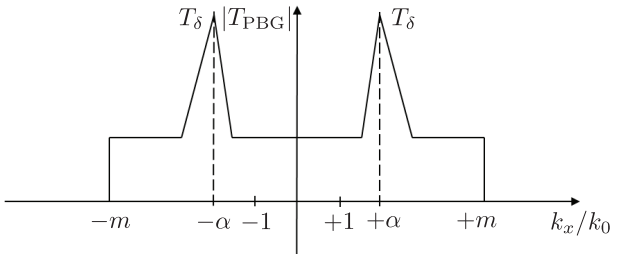

FIG. 1 Experimental and simulation results for (a) 100 μm emitter and detector antennas on LT-GaAs and (b) 200 μm emitter and detector antennas on LT-GaAs.

there is the relation $V_o(k_x) = T_{PBG}(k_x)V_i(k_x)$, where $T_{PBG}(k_x)$ is the transfer function of the linear system. If we want the output and the input field to be equal, we need the modulus of the function $T_{PBG}(k_x)$ to be constant for the entire spectral range of the input signal $V_i(k_x)$ while the phase must be constant depending on the k_x variable for the same range of space frequencies. It is clear however that it is impossible to have a constant value for the $T_{PBG}(k_x)$ function for any real k_x values [12]; there is indeed the spectral component having $k_x/k_0 = 1$ ($k_0 = 2\pi/\lambda$) and corresponding to a 90 degrees input where for any linear system we have without ambiguity $T_{PBG} = 0$; the spectral range corresponding to $|k_x/k_0| > 1$ is related to evanescent waves, and every real system has a transmission whose modulus is strongly different from zero only for a finite range of k_x. The better case of a transfer function that is able to perform a perfect reproduction of the input field at the output window is presented in Figure 1, where m is the maximum spatial frequency that the structure is able to transmit. If now we neglect the two points $k_x/k_0 = \pm 1$ (that are just two missed points in the spectrum, that gives no changing in the space domain) and the two peaks at $\pm\alpha$ which will be discussed later, we can assume that the function better reproducing the input field without effective changes is rectangularly shaped, 2 m in size and centred in the origin of the k_x axis; for the phase we suppose to have constant value in the entire range of the spectrum. If the input signal has a spectrum completely inside the rectangle, then the output reproduces exactly the shape of the field, whereas if $V_i(k_x)$ has an extension larger than the rectangle, the output signal looses the finesse of the input field at the high k_x frequencies which are cut by the transfer function of the linear system. This case is exactly what happens in the reality, where the transfer function of any PBG structure cuts the higher spatial frequencies. It is obvious that for fixed input signal the larger is the rectangle $|T_{PBG}(k_x)|$ the better will be the reproduction of the input signal. In the case of a PBG structure, it is necessary to find a geometry which has the closest transfer function to the one of Figure 1 as well and possibly with the largest rectangular base. Now we want to discuss a special transfer function that often approximates the transfer function of many 1D super resolving PBGs: it is the one represented in Figure 1 in which two peaks at some values of k_x/k_0, say $\pm\alpha$ are shown. Let us first assume that these two peaks are two Dirac-δ functions of area T_δ centred in the symmetric points $k_x/k_0 = +\alpha$ and $k_x/k_0 = -\alpha$ respectively, with $\alpha > 1$. The transfer function, disregarding the zero values at $k_x/k_0 = \pm 1$, can be described analytically as

$$T_{PBG}(k_x) = \mathrm{rect}_{2mk_0}(k_x) + T_\delta\delta(k_x - \alpha k_0) + T_\delta\delta(k_x + \alpha k_0), \quad (1)$$

where $\mathrm{rect}_T(k_x)$ is the rectangle function with base T, centred in the origin. The output field is

$$\begin{aligned} V_0(k_x) &= T_{PBG}(k_x)V_i(k_x) \\ &= \mathrm{rect}_{2mk_0}(k_x)V_i(k_x) + V_i(\alpha k_x)T_\delta\delta(k_x - \alpha k_0) \\ &\quad + V_i(-\alpha k_x)T_\delta\delta(k_x + \alpha k_0). \end{aligned} \quad (2)$$

Writing $V_i(\alpha k_0) = |V|e^{i\Phi}$ and making the inverse Fourier transformation of Eq. (2), we obtain

$$\begin{aligned} v_0(x) &= \Im^{-1}\{\mathrm{rect}_{2mk_0}(k_x)V_i(k_x)\} \\ &\quad + |V|e^{i\Phi}T_\delta e^{i\alpha k_0 x} + |V|e^{-i\Phi}T_\delta e^{-i\alpha k_0 x}, \end{aligned} \quad (3)$$

that in a more compact way can be written as

$$\begin{aligned} v_0(x) &= \Im^{-1}\{\mathrm{rect}_{2mk_0}(k_x)V_i(k_x)\} \\ &\quad + 2|V|T_\delta\cos(\Phi + \alpha k_0 x). \end{aligned} \quad (4)$$

Eq. (4) describes the electromagnetic field on the output surface of the PBG. It is the sum of two terms, the first one is the inverse Fourier transformation of the input field after cutting the high spatial frequencies ($|k_x/k_0| > m$), the second one represents an added disturb in the form of a spatial cosine at high frequency (evanescent zone because $\alpha > 1$). The field of Eq. (4) must propagate in the free space on the right of the PBG, and the evanescent frequencies drop down quickly, so the cosine is strong near the output surface of the PBG and in the x direction parallel to its face, but it drops down as well as the field propagates in the longitudinal direction: in the far field it no more survives leaving only the propagating field without evanescent components. Many 1D multilayer systems have a transfer function that may be approximated with the one described and usually with more pairs of Dirac $-\ \delta's$. We will see in fact that these frequencies are strictly linked to the geometry of the system and have no dependence from the input field. These particular spatial frequencies generate at the output, cosine terms that disturb the process of super resolving. In the following we will give more details about the physical mechanism that gives rise to these peaks in the evanescent spectrum of many PBGs. A better and more realistic situation, especially if absorption is present is the one in which the structure present spectra similar to the one we have discussed but with peaks of finite high and width as shown in Figure 1. The mathematical analysis is similar to the one we have done and the field at the output has two terms, as in Eq. (4),

$$\begin{aligned} v_0(x) &= \Im^{-1}\{\mathrm{rect}_{2mk_0}(k_x)V_i(k_x)\} \\ &\quad + [S(x)\cos(\alpha k_0 x)]\cdot v_i(x). \end{aligned} \quad (5)$$

The first term is still the inverse Fourier transformation of the input electromagnetic field after cutting high spatial frequencies with $|k_x/k_0| > m$ (this term takes into account the loss of high spatial frequencies). The second term is a convolution between the cosines with a function $S(x)$ (that is the Fourier transform of the peaks at $\pm\alpha$ shown in the figure) which is due to the finite sizes of the peaks and gives an oscillatory symmetric function that decays with increasing $|x|$. In this case too, the peaks add a disturb to the output signal but now span only for a limited extension on the x axis. If for example as input signal we use a rectangular function along x then the output field, due to the first term in Eq. (5) will still be almost rectangular (the high spatial frequencies

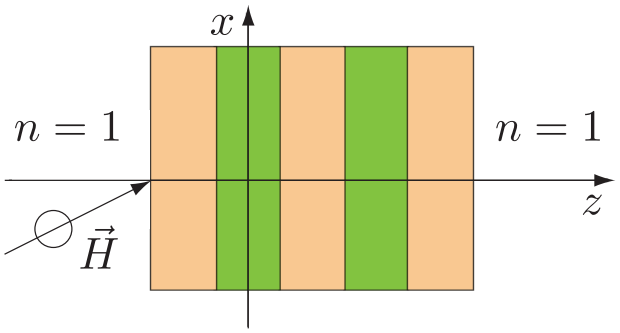

FIG. 2 Special case of a metal-dielectric PBG with five layers, the two metal layers are filled by silver while the three dielectric ones are without absorption and with refractive index $n_d = 4$.

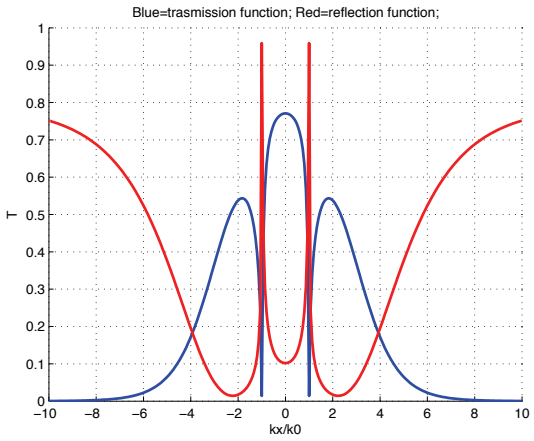

FIG. 3 Plot of the transmission and reflection spectra.

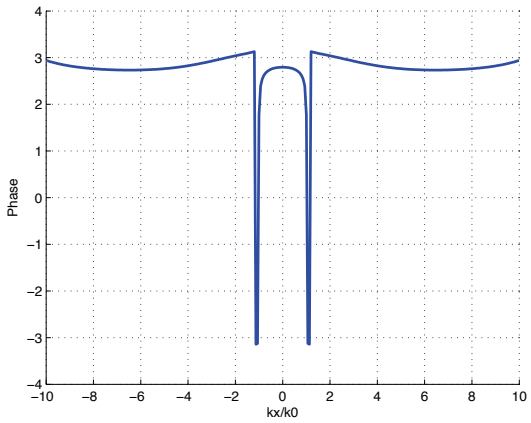

FIG. 4 Plot of the transmission and reflection spectra.

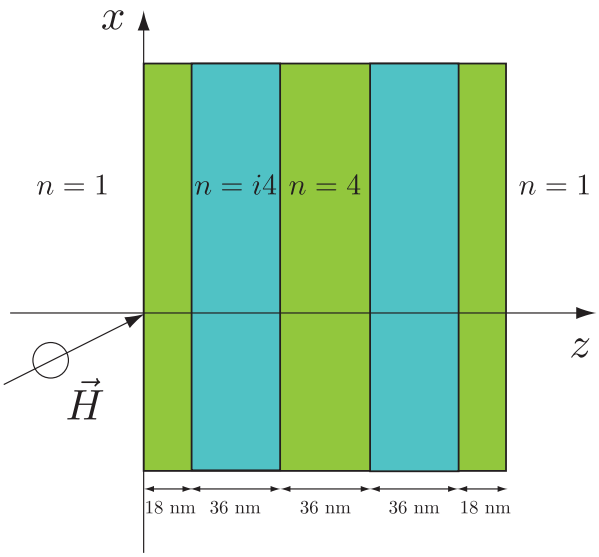

FIG. 5 A lossless and no dispersive metal-dielectric PBG with five layers.

are cut from the transfer function) superposed with a function that oscillates from the origin reducing as $|x|$ increases. This is what happens on the output surface. If we consider the propagation of the field in the z direction, all the evanescent oscillatory components decay very soon leaving just the propagating field. It is clear from this discussion that the more are the peaks the more is the disturb at the output. We show now an example taking into account a particular PBG. In Figure 2 a metal-dielectric PBG with five layers is shown (two filled by metal and three with dielectric), the metal is silver while the dielectric is without absorption and with refractive index $n_d = 4$. The wavelength is $\lambda = 0.600$ μm and for the silver we take $n_{Ag} = 0.1243 + i3.7316$. The polarization is TM. The thickness of all the layers is 20 nm, so the whole PBG is thick 100 nm. The transmission and reflection spectra are shown in Figure 3 while the phase is shown in Figure 4. The transmission spectrum has a finite band-width extending approximately from -6 to $+6$ k_x/k_0 with three broaden maxima: one in the real zone between $|k_x/k_0| < 1$ and two symmetric around $k_x/k_0 = \pm 2$. The phase is almost constant in the evanescent zone $|k_x/k_0| > 1$ as it should be in order to reproduce a perfect copy of the input signal. Usually this kind of phase, almost constant in the spectral range of a large band, occurs quite regularly in the systems we are studying.

3 IS IT POSSIBLE TO ENLARGE THE k_x SPECTRUM?

In this Section we want to give a physical explanation of the broad peaks as the ones shown in Figure 3, that are typically present in multilayer structures in the evanescent zone: they may be associated to the presence of real modes propagating in the direction parallel to the multilayer planes. We start studying an ideal case, and after we will extend our results to real cases.Without loss of generality we may consider the PBG plotted in Figure 5. The polarization is TM. The multilayer can be seen in the z direction as an open resonator, in which some modes exist. The mathematical analysis to find the modes follows exactly the one used in optical guides in which light propagates in the x direction; the guides indeed in the transverse direction are resonators. From the study of the modes inside the guide [13] we can find the dispersion curves that link the modes to the couple of values k_x and λ. The dispersion curve for the system of Figure 5 is shown in Figure 6 (it appears discretized just due to the representation technique). In this example, below $\lambda = 0.5$ μm there are no more dispersion curves. In Figure 6 we analyze only the window $k_x/k_0 > 1$ because the modes must be evanescent outside the PBG [13].

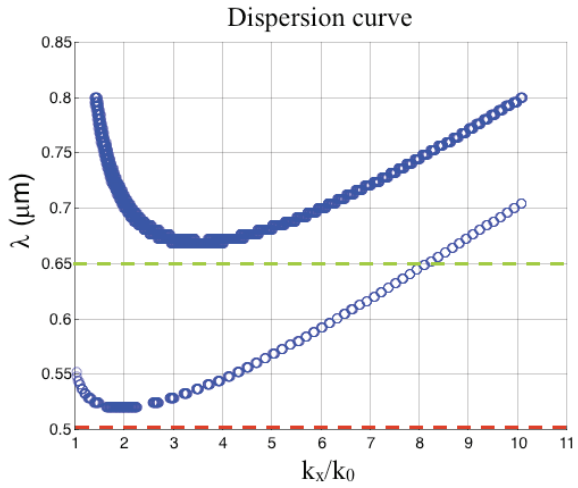

FIG. 6 Dispersion curve for the system of Figure 5.

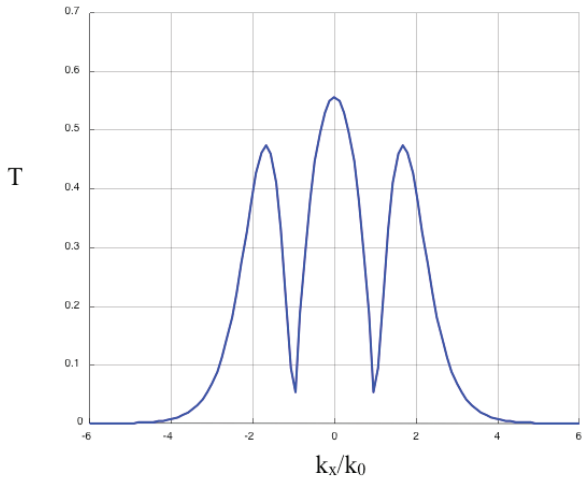

FIG. 7 Angular transmission for the system of Figure 5.

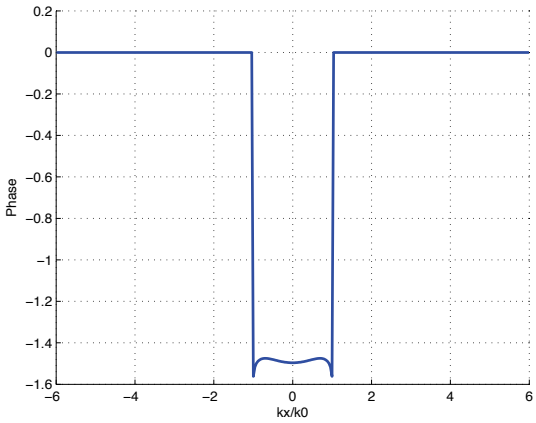

FIG. 8 Phase for the system of Figure 5 at $\lambda = 0.5\ \mu$m.

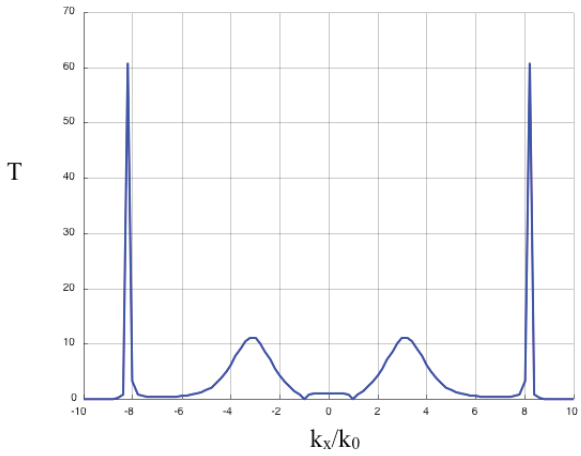

FIG. 9 Angular transmission for the system of Figure 5 at $\lambda = 0.65\ \mu$m.

If we excite the PBG with a plane wave, at $\lambda = 0.5\ \mu$m with a generic k_x (red dashed line in Figure 6), we are not able to exactly excite any mode but, because we are very close to the resonant dispersive curve at $\lambda = 0.52\ \mu$m with $k_x/k_0 \simeq 2$, the field inside the resonator may grow somehow and with it the evanescent tails outside the multilayer will grow. In Figure 7 we show the angular transmission for $\lambda = 0.5\ \mu$m while in Figure 8 we plot the phase that appear constant for the large range of the spectrum. For the range of values k_x/k_0 that are closer to the dispersion curve, say $1 < k_x/k_0 < 3$, there is a very broad transmission without peaks (there are no peaks because we are not exactly exciting modes at $\lambda = 0.52\ \mu$m). If we now select the wavelength at $\lambda = 0.65\ \mu$m (green dashed line in Figure 6) we should have a broad transmission inside the range $2 < k_x/k_0 < 5$ while a mode at $k_x/k_0 \simeq 8$ (that is the interSection between the green dashed line and the dispersion curve) could be stimulated which generates a peak in the spectrum exactly at this value (see Figure 8). We have only to underline that the peaks are not very high just because computing discretization was low, but here because we have no absorption and the mode is stimulated we should have an infinite amplitude peaks. In Figure 9 we plot the dispersion curve for the system of Figure 5 but for TE polarization. In this case for every wavelength there is at least one k_x value that intersect the wavelength line we are working with; so it is impossible in this case to generate a simple broadening of the band without peaks in the spectrum. In Figure 10 we show the case where $\lambda = 0.600\ \mu$m. We have a peak at $k_x/k_0 \simeq 1.3$ that is exactly the interSection between the dashed red line and the dispersion curve of Figure 9. Let now consider the same structure of Figure 5 in which now the two layers with $n = i4$ are substituted with two metal layers with $n = 1 + i4$. We choose a high real value just to test the goodness of the theory. After we will study a realistic metal-dielectric multilayer made with silver. The polarization is TM. If we analyze the dispersion curve we obtain the curve of Figure 11. Before proceeding further, we have to explain how it was obtained and which are the differences with the dispersion curve of the previous system. From the theory of a wave guide [13] described by a 2×2 transmission matrix, we know that to find the guided modes it is necessary that the element $m_{22}(k_x, \lambda)$ of this matrix satisfies the relation

$$m_{22}(k_x, \lambda) = 0. \tag{6}$$

From Eq. (6) it is possible to find all possible modes that can travel inside the guide. For the lossless case Eq. (6) has roots just because there are modes that can survive for an infinite time inside the cavity of the waveguide, but if losses are present Eq. (6) cannot be satisfied (inside the cavity there are no modes that can survive for an infinite time). In this case the function $m_{22}(k_x, \lambda)$ can just be close to zero but without

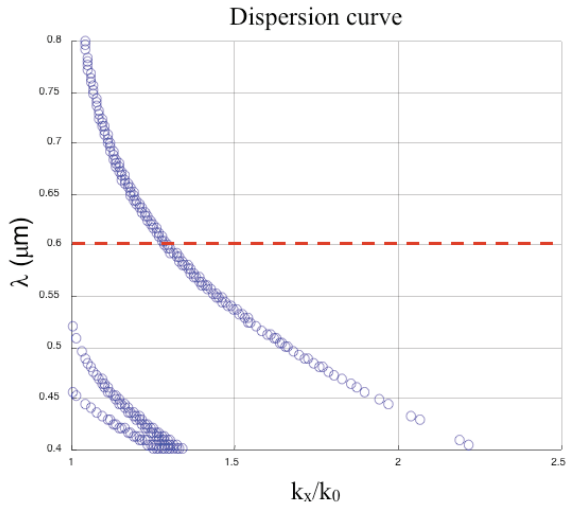

FIG. 10 Dispersion curve for the system of Figure 5.

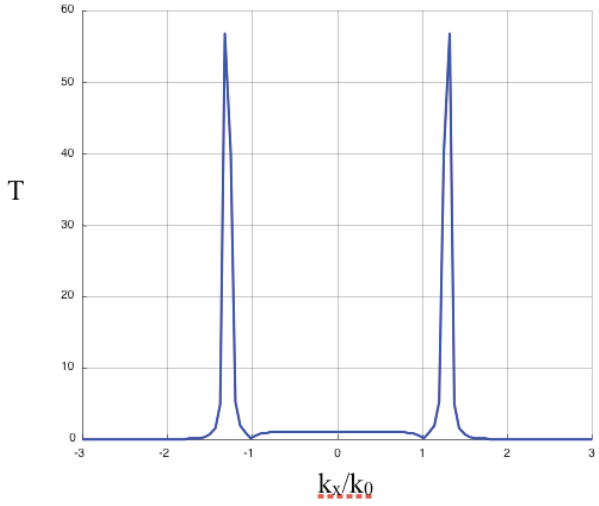

FIG. 11 Angular transmission for the system of Figure 5 at $\lambda = 0.6\ \mu$m.

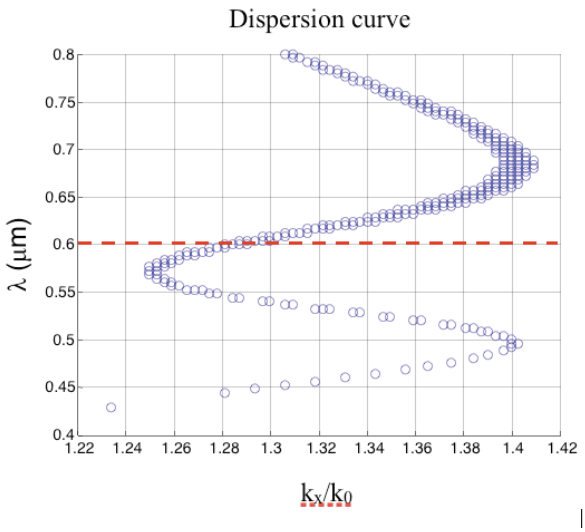

FIG. 12 Dispersion curve for the system of Figure 5 substituting the materials $n = i4$ with others having $n = 1 + i4$.

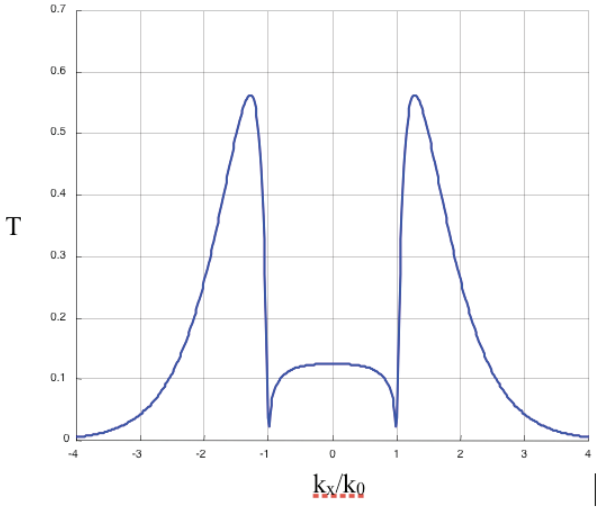

FIG. 13 Angular transmission for the system of Figure 5 at we substituted the materials $n = i4$ with others having $n = 1 + i4$.

reaching it. The case of absence of roots for Eq. (6) is exactly the situation of the PBG with losses, the real modes do not exist anymore but there are points of resonance (the minima of the function $|m_{22}(k_x, \lambda)|$) where we can increase the field inside the cavity at values much higher than the input. In Figure 11 we plotted all the minima of the function $|m_{22}(k_x, \lambda)|$.

It is clear that the larger are the losses of the system the more distant are the minima from zero and the weaker are the corresponding resonances. In Figure 12 we plot the angular transmission at $\lambda = 0.6\ \mu$m. In this case the dashed line at $\lambda = 0.6\ \mu$m in Figure 11 intersect the dispersion curve but as we can see from Figure 12 the transmission grows keeping it limited and generating a smoothed peak exactly in the interSection point ($\lambda = 0.6\ \mu$m, $k_x/k_0 = 1.28$). This limited and smoothed peak at interSection is due to the fact we are no more in presence of a real mode but just of a resonance, where the losses limit the field amplitude inside and outside the cavity. In Figure 13 the dispersion curve for the same system is plotted for TE polarization. In this case too we always intersect the dispersion curves, but here too due to losses we have a broadening enlarging the transmission spectrum without peaks. This is seen in Figure 14 in which the transfer function for $\lambda = 0.6\ \mu$m is plotted. A band with the maximum at $k_x/k_0 \simeq 1.21$) that corresponds to the interSection between the dashed line with the dispersion curve, Figure 13 is seen. The conclusion is that the broad peaks that appear in the spatial spectrum of the multilayer structure for $|k_x/k_0| > 1$ correspond to the evanescent tail of transverse wave propagating parallel to the multilayer planes which can be excited from outside.

4 DESIGN RULES FOR LARGE BAND PBG

In this Section we want to discuss some ideas for designing metal-dielectric 1D-PBG with large band and good transmission over the entire spectral range. We analyze for the moment only symmetric systems, we chose a multilayer structure with alternating metal and dielectric layers with the following sequence $DMDMDMDMDMDMD$ where D is a dielectric and M is a metal, all the dielectric layers are equal, all the metal layers are equal too, in input and output of the structure we have the vacuum. All the dielectric layers have the same thick-

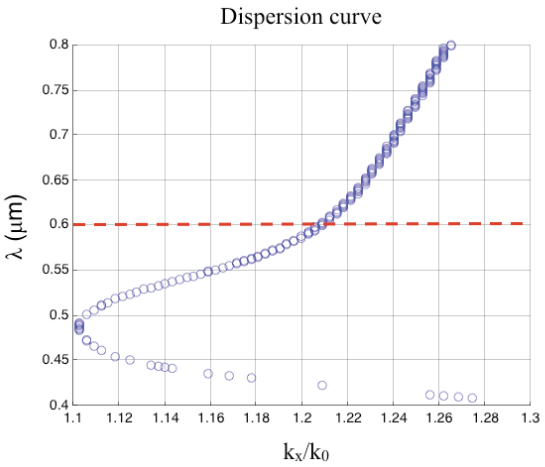

FIG. 14 Dispersion curve for the system of Figure 5 substituting the materials $n = i4$ with others having $n = 1 + i4$.

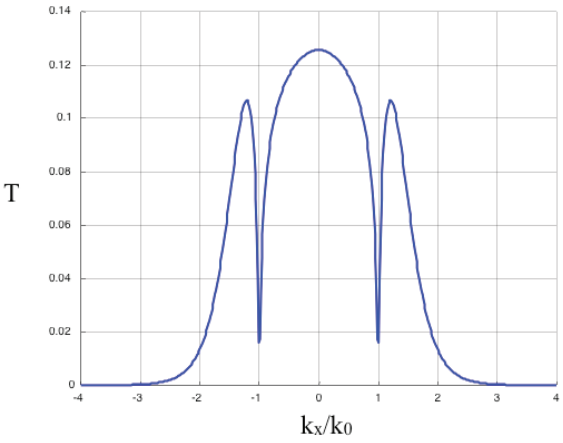

FIG. 15 Angular transmission for the system of Figure 5 at $\lambda = 0.6$ μm, we substituted the refractive index of the metal $n = i4$ with $n = 1 + i4$.

ness d_d and refractive index n_d, all the metal layers have the same thickness d_m and refractive index n_m while the polarization is TM. In the analysis we have to search a geometry that is able to enlarge the band without generating peaks in the spectrum. First we fix the wavelength at the value λ_0 where the dielectric refractive index and the imaginary part of the metal refractive index are equal (or in any case very close to each other), so we need that

$$n_d(\lambda_0) = \mathrm{Im}\{n_m(\lambda_0)\} \tag{7}$$

and we choose a metal where the real part of the refractive index is very low with respect to the imaginary one,

$$Re\{n_m(\lambda_0)\} << \mathrm{Im}\{n_m(\lambda_0)\}. \tag{8}$$

An ideal metal for which $\mathrm{Re}\{n_m(\lambda_0)\} = 0$ would be the best choice, but if the real part of the metal refractive index is very low compared with the imaginary one, all the discussion in the following is still valid. The reasons for these choices will be explained later. Now we apply Eqs. (7) and (8) to a real case. We choose $\lambda = 388$ nm , in this region the silver has a refractive index $n_m = 0.1824 + i1.8164$. Therefore we choose a dielectric with refractive index around 1.8 at $\lambda = 388$ nm. We choose six silver and seven dielectric layers to build our

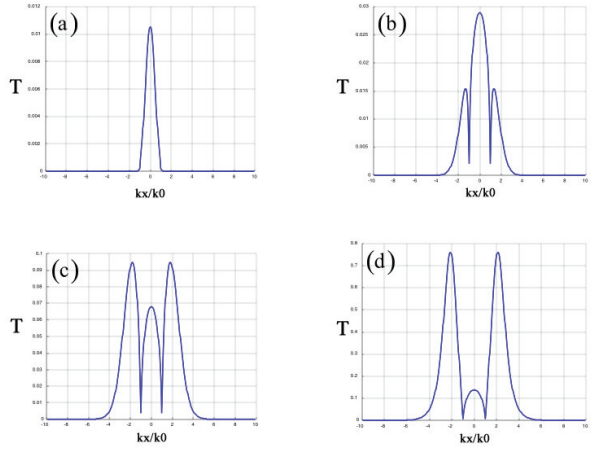

FIG. 16 Angular transmission spectrum for the metal-dielectric system at $\lambda = 388$ nm, $n_d = 1.8$ and a) $d_d = d_m = 60$ nm, b) $d_d = d_m = 30$ nm, c) $d_d = d_m = 20$ nm, d) $d_d = d_m = 15$ nm.

PBG. To start with we fix all the thicknesses of the layers equal to each other and rather large, for example we can start with $d_d = d_m = 60$ nm and then we decrease the thickness of the layers to see which is their influence on the transmission spectrum. Several cases are shown in Figure 16, which shows the angular spectrum for different values of the thickness. We see that, with the large thickness we have chosen to start with, the angular spectrum of the system is regular (without resonances), narrow and with a very low transmission value (Figure 16(a)). Reducing the thickness of the layers, the spectrum starts to open. For $d_d = d_m = 30$ nm (Figure 16(b)) and $d_d = d_m = 20$ nm (Figure 16(c)), the spectrum is rather broadened. For $d_d = d_m = 15$ nm (Figure 16(d)) we see that the modulus of the propagating waves reaches a maximum value of about 15% in transmission while the evanescent components still grow. For smaller thicknesses we increase the resonances of the evanescent field but the transmission spectrum is no more uniform. So we may decide to stop the thickness of the layer at about 20 nm just diversifying a little bit the thickness of the metal from the dielectric to find a more uniform transmission. We choose 18 nm for the dielectrics and 20 nm for the metal and finally we have the spectrum of Figure 17(a) which has a low modulus but a spectral width larger than $k_x/k_0 = 4$. In Figure 17(b) the dispersion curve is plotted. The dashed line ($\lambda = 388$ nm) intersect the curve at about $k_x/k_0 = 2$ where there is the maximum of the transmission, the peaks are not infinite just because there is the absorption of the silver. Now we show how important is to have the condition (8) well verified. We modify the refractive index of the silver to $n_m = 0 + i1.8164$. The spectrum of Figure 17(a) modifies in the one of Figure 18(a) showing a very large width which demonstrates that this system with ideal metal and symmetric geometry is able to avoid the resonance peaks and to super resolve a signal large at minimum 1/10 of the wavelength. The good behavior of the phase is shown in Figure 18(d). From this example we see that it is not important to have a very large refractive index for the dielectric to have a large band in the spectrum but it is important that Eqs. (7) and (8) are well verified. In Figure 18(b) the dispersion curves are plotted and one of them is tangent to the line $\lambda = 388$ nm (dashed line); just because the discretization is

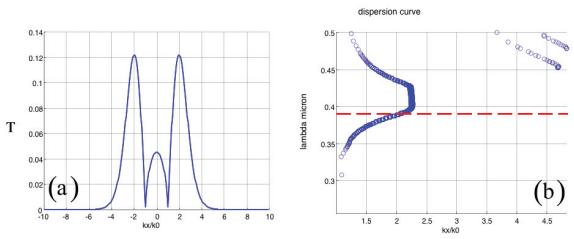

FIG. 17 a) angular transmission spectrum for the metal-dielectric system where $d_d = 18$ nm, $d_m = 20$ nm, $n_d = 1.8$, $\lambda = 388$ nm. b) dispersion curve.

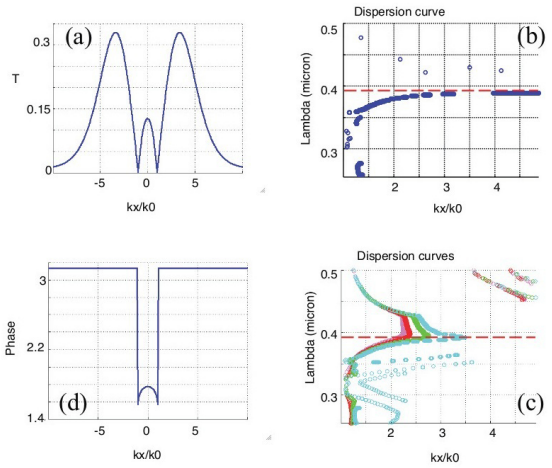

FIG. 18 a) angular transmission spectrum d) phase spectrum, for the metal-dielectric system where $d_d = 18$ nm, $d_m = 20$ nm, $n_d = 1.8$, $n_m = 0 + i1.8164$, $\lambda = 388$ nm. b) dispersion curve. c) dispersion curves calculated for different values of the real part of the silver refractive index: Pink: $n_{Ag} = 0.1824$, Red: $n_{Ag} = 0.1500$, Green: $n_{Ag} = 0.1000$, Blue: $n_{Ag} = 0.0500$ where k_{Ag} is always 1.8164.

low the dispersion curve up to the line $\lambda = 388$ nm is plotted with a few points and the tangent curve appears broken, but it is continue. In Figure 18(c) the dispersion curves are plotted always for the same system but changing the real part of the silver refractive index. We can see that just for completely absence of absorption (Figure 18(b)) the dispersion curve is tangent to the line $\lambda = 388$ nm , for all other cases we cannot avoid the interSection with almost one dispersion curve. This characteristic is completely general, when absorption is present, it is never possible to avoid the interSection between the line $\lambda = const$ and the dispersion curves. We analyzed many others structures using different types of systems, both symmetric or non-symmetric, and also studying all-dielectric PBGs. We observed that in the case of all-dielectric systems the polarization that better works to broaden the band is TE while usually for TM there are strong peaks close to the points $k_x/k_0 = \pm 1$. In the case of all-dielectric PBG the maximum width we may have in the band is given from the maximum refractive index difference between the layers. Moreover we may have a nearly uniform spectrum just if we have some losses, the interSection between $\lambda = const$ and the dispersive curves are indeed impossible to avoid in any case.

5 CONCLUSIONS

From the presented discussion one may infer that the super resolution for thick multilayer system is a phenomenon that can be completely explained as a resonant effect. It is due to the resonances inside the PBG which in the propagation direction may be seen as an open cavity. Considering the resonator representation with the resonant points, we may explain why there are often strong peaks in the angular spectrum and only in the evanescent zone; we may also easily explain the phenomenon of the uniform band broadening, linking it to the dispersion curves and the quasi resonant regimes inside the PBG cavity. We also showed that it could be possible to obtain large bands for both TE and TM polarization. The all-dielectric 1D multilayer structure although in principle could work needs more investigation to be done in a further work. We demonstrated that to have very large bands it is necessary to respect as better as it is possible the conditions 7 and 8, without having very large refractive index in the layers. The phase behavior of all the studied systems keeps almost constant in the range of interest which assures a good response. There is only a discontinuity at $k_x/k_0 = 1$ and a jump from the region $|k_x/k_0| \leq 1$ and $|k_x/k_0| > 1$ which can be accounted for in the reconstruction process.

6 ACKNOWLEDGEMENTS

The authors wish to acknowledge discussion with M. Scalora and C. Sibilia.

References

[1] J. B. Pendry, “Negative refraction makes a perfect lens” Phys. Rev. Lett. **85**, 3966–3969 (2000).

[2] N. Fang, H. Lee, C. Sun, and X. Zhang, “Sub-diffraction-limited optical imaging with a silver superlens” Science **308**, 534–537 (2005).

[3] D. O. S. Melville, R. J. Blaikie, C. R. Wolf, “Super-resolution imaging through a planar silver layer” Opt. Express **13**, 2127–2134 (2005).

[4] E. Betzig and R. J. Chichester, “Single molecules observed by near-field scanning optical microscopy” Science **262**, 1422–1425 (1993).

[5] P. N. Prasad, *Nanophotonics*, Chapter 3 (1st Edition. John Wiley & Sons, Hoboken, 2004).

[6] X. Li, S. He, and Y. Jin “Subwavelength focusing with a multilayered Fabry-Perot structure at optical frequencies” Phys. Rev. B **75**, 045103 (2007)

[7] S. A. Ramakrishna, J. B. Pendry, M. C. K. Wiltshire, W. J. Stewart, J. Mod. Opt. **50**, 1419–1430 (2003).

[8] J. B. Pendry, and S. A. Ramakrishna, “Refining the perfect lens” Physica B **338**, 329–332 (2003).

[9] B. Wood, J. P. Pendry, and D. P. Tsai, “Directed sub-wavelength imaging using metal-dielectric system” Phys. Rev. B **74**, 115–116 (2006).

[10] P. A. Belov, and Y. Hao, “Subwavelength imaging at optical frequencies using a transmission device formed by a periodic layered metal-dielectric structure operating in the canalization regime” Phys. Rev. B **73**, 110–113 (2006).

[11] M. Scalora et al, “Negative refraction and sub-wavelength focusing in the visible range using transparent metal dielectric stacks”

Opt. Express **15**, 508–523 (2007).

[12] H. M. Nussenzveig, *Causality and Dispersion Relations* (Academic Press, New York, 1972).

[13] R. E. Smith, S. N. Houde-Walter, and G. W. Forbes, "Mode determination for planar waveguides using the four-sheeted dispersion relation" IEEE J. Quantum Elect. **28**, 1520–1526 (1992).